Lattice-tuned magnetism of Ru^{4+}(4d^{4}) ions in single crystals of the layered honeycomb ruthenates Li_{2}RuO_{3} and Na_{2}RuO_{3}

J. C. Wang, J. Terzic, T. F. Qi, Feng Ye, S. J. Yuan, S. Aswartham, S. V. Streltsov, D. I. Khomskii, R. K. Kaul, and G. Cao

Lattice-Tuned Magnetism of Ru^{4+}(4d^4) Ions in Single-Crystals of the Layered Honeycomb Ruthenates: Li$_2$RuO$_3$ and Na$_2$RuO$_3$

J. C. Wang[1,2,3], J. Terzic[1], T. F. Qi[1], Feng Ye[2,1], S. J. Yuan[1,4], S. Aswartham[1], S. V. Streltsov[5,6], D. I. Khomskii[7], R. K. Kaul[1] and G. Cao[1*]

[1]Center for Advanced Materials, Department of Physics and Astronomy, University of Kentucky, Lexington, KY 40506, USA

[2]Quantum Condensed Matter Division, Oak Ridge National Laboratory, Oak Ridge, Tennessee 37831, USA

[3]Department of Physics, Renmin University of China, Beijing, China

[4]Department of Physics, Shanghai University, Shanghai, China

[5]Institute of Metal Physics, 620041 Ekaterinburg, Russia

[6]Ural Federal University, 620002 Ekaterinburg, Russia

[7]II.Physikalisches Institut, Universitaet zu Koeln, Germany

We synthesize and study single crystals of the layered honeycomb lattice Mott insulators Na$_2$RuO$_3$ and Li$_2$RuO$_3$ with magnetic Ru^{4+}(4d^4) ions. The newly found Na$_2$RuO$_3$ features a nearly ideal honeycomb lattice and orders antiferromagnetically at 30 K. Single-crystals of Li$_2$RuO$_3$ adopt a honeycomb lattice with either C2/m or more distorted P2$_1$/m below 300 K, depending on detailed synthesis conditions. We find that Li$_2$RuO$_3$ in both structures hosts a well-defined magnetic state, in contrast to the singlet ground state found in polycrystalline Li$_2$RuO$_3$. A phase diagram generated based on our results uncovers a new, direct correlation between the magnetic ground state and basal-plane distortions in the honeycomb ruthenates.

PACS: 75.10.Jm, 75.25.Dk, 75.40.-s

Introduction It has been of great interest to study interacting electrons on the honeycomb lattice in various contexts both experimentally (e.g. graphene) and theoretically (e.g the Kitaev model). Studies of honeycomb materials have intensified in recent years [1-19] in part because strong spin-orbit coupling (SOC) along with other competing interactions and geometric frustration in the honeycomb iridates Na_2IrO_3 and Li_2IrO_3 favors a highly anisotropic Kitaev interaction [20] that stabilize exotic ground states such as topological spin-liquids [1]. It is now experimentally established that Na_2IrO_3 exhibits a peculiar zigzag magnetic order at T_N=18 K [5, 14, 15], and Li_2IrO_3 also orders at T_N=15 K but with a different ground state yet to be defined [3, 17, 21, 22, 23]. Indeed, for $(Na_{1-x}Li_x)_2IrO_3$ with $0 \leq x \leq 0.90$, the measured phase diagram demonstrates a dramatic suppression of T_N at intermediate x suggesting that the magnetic order in Na_2IrO_3 and Li_2IrO_3 is different; however, no spin liquid has been observed thus far [17]. Our pursuit of an understanding of the honeycomb iridates has led us to their ruthenate counterparts, Na_2RuO_3 and Li_2RuO_3. These materials feature $Ru^{4+}(4d^4)$ ions and a weaker or "intermediate strength" SOC (~ 0.16 eV, compared to ~ 0.4 eV for Ir ions) [24]. The different d-shell filling and contrasting hierarchy of energy scales between the ruthenates and iridates provide a unique opportunity for a deeper understanding of the fundamental problem of interacting electrons on the honeycomb lattices. The magnetism of Ru^{4+} ions as well as other heavy "d^4 ions" (such as $Rh^{5+}(4d^4)$, $Re^{3+}(5d^4)$, $Os^{4+}(5d^4)$ and $Ir^{5+}(5d^4)$) is interesting in their own right, as emphasized recently [25]. Materials with heavy d^4 ions tend to adopt a low-spin state because larger crystal fields often overpower the Hund's rule coupling. On the other hand, SOC with the intermediate strength may still be strong enough to impose a competing, singlet ground

state or an angular momentum J=0 state. Novel magnetic states may thus emerge when the singlet-triplet splitting (0.05-0.20 eV) becomes comparable to exchange interactions (0.05-0.10 eV) and/or non-cubic crystal fields [25-27]. This is evidenced in a recent study of materials containing $5d^4$ ions [28].

Up until now, no physical and structural properties of Na_2RuO_3 have been investigated but a few experimental and theoretical studies of polycrystalline Li_2RuO_3 have been reported in recent years [29-32]. In essence, polycrystalline Li_2RuO_3 undergoes a structural phase transition near T_D=540 K that features a change of space group from C2/m (No. 12) at high temperatures to $P2_1/m$ (No. 11) at low temperatures. The low-temperature phase adopts a strongly distorted honeycomb lattice, which prompts a simultaneous dimerization that results in a singlet ground state [29]. The observation of dimerized zigzag chains has recently stimulated more investigations of Li_2RuO_3 [30-32], in which the dimerization is attributed to orbital ordering [29], creation of valence bond crystal [30] and Jahn-Teller distortions [31], respectively. It is noted that all reported experimental results were culled from polycrystalline Li_2RuO_3 [29, 31, 32].

Here we report structural, magnetic, and thermal properties of single-crystal Li_2RuO_3 and Na_2RuO_3. The newly found Na_2RuO_3 with space group C2/m features a nearly ideal honeycomb lattice and orders antiferromagnetically below 30 K. It may serve as a reference for almost perfect honeycomb symmetry. On the other hand, single-crystal Li_2RuO_3 adopts a less ideal honeycomb lattice with either C2/m or more distorted $P2_1/m$ below 300 K but both phases exhibit a well-defined, though different, magnetic state, which sharply contrasts with the singlet ground state due to dimerization observed in polycrystalline Li_2RuO_3 [28]. This work produces a phase diagram that uncovers a direct

correlation between the ground state and basal-plane distortions or lattice-tuned magnetism in all honeycomb ruthenates studied. (Both Li_2RuO_3 and Na_2RuO_3 are highly insulating; their transport properties are not included in this paper.)

Crystal Structures Single-crystals of Li_2RuO_3 and Na_2RuO_3 were synthesized using the self-flux method, which is described elsewhere [17]. For synthesis of single-crystal Li_2RuO_3 the mixed chemicals were first heated up to 1250 ^{o}C and then cooled to 900 ^{o}C at 2 ^{o}C/hour and finally room temperature at 50 ^{o}C/hour. In contrast, the polycrystalline Li_2RuO_3 was synthesized at much lower temperature of 950 ^{o}C. The different synthesis conditions may have important implications for the ground state of Li_2RuO_3. For more experimental details, see Supplemental Material [33]. Crystal structures on which the ground state so sensitively hinges require a close examination. **Table 1** includes the lattice parameters of single-crystals Li_2RuO_3 and Na_2RuO_3 as well as those of polycrystalline Li_2RuO_3 and iridate counterparts for contrast and comparison. For the sake of discussion, single-crystal Li_2RuO_3 with C2/m and $P2_1$/m are labeled as Li_2RuO_3 (C) and Li_2RuO_3 (P), respectively. A major distinction between Li_2RuO_3 (C) and Li_2RuO_3 (P) is the number of unequal Ru-Ru bond distances, which measures distortions that in turn dictate the ground state. Li_2RuO_3 (C) features two bond distances, or a long and short one, L_l and L_s, respectively, whereas Li_2RuO_3 (P) has three bond distances, i.e., L_l, L_s, and a medium bond distance, L_m. The basal-plane distortion is characterized by the bond difference ratio defined as $(L_l-L_s)/L_s$, which is shown in **Table 1**, **Figs 1a** and **1b**. In general, honeycomb lattices with C2/m tend to have a larger a-axis lattice parameter and smaller ratio b/a ($\sim\sqrt{3}$) than those with $P2_1$/m, thus less distorted. **Figs.1c** and **1d** demonstrate the lattice parameters of single-crystal and polycrystalline samples as a

4

function of temperature. As seen, no structural transition is discerned in the single crystals studied for the temperature range measured. *In short, the structural differences between the polycrystalline Li$_2$RuO$_3$ and Li$_2$RuO$_3$ (C) or Li$_2$RuO$_3$ (P) are distinguished by the different space groups or by the difference in (L_l-L_s)/L_s. It is clear that Li$_2$RuO$_3$ (P) is more distorted than Li$_2$RuO$_3$ (C) but much less distorted than the polycrystalline sample despite the same space group shared by both* **(Table 1)**.

Table 1. Structural comparison between the honeycomb lattices at 100 K

Compound	Space Group	a (Å)	b (Å)	b/a	(L_l-L_s)/L_s
Li$_2$RuO$_3$ (Powder)*	P2$_1$/m	4.9210(2)	8.7829(2)	1.785	18.6%
Li$_2$RuO$_3$ (P)	P2$_1$/m	4.963(3)	8.766(6)	1.766	10.1 %
Li$_2$RuO$_3$ (C)	C2/m	5.021(4)	8.755(6)	1.744	2.1 %
Na$_2$RuO$_3$	C2/m	5.346(1)	9.255(2)	1.731	0.17 %
(Li$_{0.9}$Na$_{0.1}$)$_2$IrO$_3$	C2/m	5.186(1)	8.964(2)	1.728	0.6 %
Na$_2$IrO$_3$	C2/m	5.319(1)	9.215(2)	1.732	0.14 %

* Taken at 300 K

Physical Properties Na$_2$RuO$_3$ exhibits a sharp antiferromagnetic (AFM) transition at T$_N$=30 K, as shown in **Fig. 2a**. The magnetic anisotropy leads to a stronger out-of-plane magnetic susceptibility $\chi_\perp$ than in-plane magnetic susceptibility $\chi_\parallel$. The linearity illustrated in 1/$\Delta\chi_\parallel$ (right scale in **Fig. 2a**) indicates that the data fit well with the Curie-Weiss law for 100 < T <350 K, and yield the Curie-Weiss temperature θ_{CW} = -137 K and effective moment μ_{eff} = 2.45 μ_B/Ru (**Table 2**). The frustration parameter defined as FP = |θ_{CW}|/T$_N$ is estimated to be 4.6. This value suggests a presence of modest frustration, comparable to that for its iridate counterpart.

The magnetic ordering is confirmed by the specific heat C(T) (**Fig. 2b**). However, an additional peak at T$_{N2}$ = 26 K that is absent in χ(T) is also seen in C(T). This behavior, which is reproducible, is remarkably similar to that observed in Na$_2$IrO$_3$ where an additional, weaker anomaly in C(T) is discerned at T* = 21 K that is followed by the

zigzag order at $T_N = 18$ K [15, 17]. This two-step transition is discussed in context of the Kitaev-Heisenberg model on the hexagonal lattice [34]. A similar argument could be applied to Na_2RuO_3 although the origin of this magnetic behavior needs to be further investigated. The C(T) data also indicate that the entropy removal due to the two-step magnetic transition is small, less than 10% of Rln3 expected for an S=1 magnet. This implies that the magnetic ordering may not be fully developed perhaps in part because of the tendency of SOC to impose a singlet state. Application of magnetic field up to 14 T causes no visible changes in both C(T,H) and χ(T,H).

Table 2. Physical parameters of the *single-crystal* honeycomb lattices

Compound	T_N	θ_{CW}	FP	μ_{eff} (μ_B/Ru or Ir)
Li_2RuO_3 (P)	~ 5	-58	11.6	1.46
Li_2RuO_3 (C)	9	-112	12.4	2.77
Na_2RuO_3	30	-137	4.6	2.45
$(Li_{0.9}Na_{0.1})_2IrO_3$	7	-18	2.6	1.95
Na_2IrO_3	18	-119	6.6	1.76

FP stands for frustration parameter

The magnetic properties of both single-crystal Li_2RuO_3 (C) and Li_2RuO_3 (P) are examined for $1.7 < T < 900$ K. Neither shows the singlet ground state observed in the polycrystalline Li_2RuO_3. Instead, Li_2RuO_3 (C) displays paramagnetic behavior at $T > 20$ K with the magnetic susceptibility χ following the Curie-Weiss law for 20 K $< T \leq 750$ K (**Fig.3a**). Data fits to the Curie-Weiss law yield an effective moment $\mu_{eff} = 2.77$ μ_B/Ru, consistent with that expected for an S=1 system, and a Curie-Weiss temperature θ_{CW}=-112 K. A signature for a long-range order near $T_N = 9$ K is evident in both χ(T) and C(T) (**Fig. 3b**). A large frustration parameter, FP $= |\theta_{CW}|/T_N = 12.4$ suggests the presence of significant frustration (**Table 2**). Indeed, the two unequal Ru-Ru bonds may favor a formation of zigzag chains along the a-axis (see schematic in the inset of **Fig. 4**) as the inter-chain interaction is weak due to the long Ru-Ru bond L_l. Therefore, no magnetic

ordering occurs until below $T_N = 9$ K when three-dimensional correlations are established.

For more distorted Li_2RuO_3 (P), a magnetically ordered state also takes place but at a lower temperature, $T_N = 4$ K (**Fig. 3c** and **3d**). Remarkably, the magnetic anisotropy is much stronger, and the magnitude of $\chi_\perp$ is significantly larger than that in Li_2RuO_3 (C), implying the importance of SOC. However, the temperature dependence of χ at high temperatures is much weaker than that for Li_2RuO_3 (C). The results suggest that Li_2RuO_3 (P) is "half-way" to dimerization as the lattice is more similar to that of the polycrystalline sample; the magnetic state eventually prevails below $T_N = 4$ K because Li_2RuO_3 (P) is after all not as distorted as the polycrystalline Li_2RuO_3.

Computational Results Our LDA (local density approximation) calculations using the LMTO (linearized muffit-tin orbitals) method [35] and Wannier function projection method [36] show that the crystal-field splitting in the Ru t_{2g} shell does not exceed 70 meV, indicating that the comparable SOC may play a significant role. However, the off-diagonal matrix elements of the Hamiltonian, hopping parameters, are even larger, ~ 200 meV, which is strong enough to form the quasi-molecular orbitals (QMOs) similar to those in Na_2IrO_3 where QMOs involve six Ir atoms arranged in a hexagon and each Ir atom belongs to three different QMOs, which dominate the formation of electronic structure [13]. The results of the optimization of the crystal structure performed in the GGA (generalized gradient approximation) calculations using the pseudopotential method [37] indicate that the nearly ideal honeycomb Na_2RuO_3 indeed corresponds to a minimum of the total energy for an AFM state. In addition, our GGA+U calculations show that a relatively small on-site Coulomb repulsion U ~ 1.5 eV is sufficient to

suppress the dimerization observed in polycrystalline Li_2RuO_3. The band structure of single-crystal Li_2RuO_3 strongly differs from that of both Na_2RuO_3 and Na_2IrO_3 on the LDA level (**see SM Fig. 2 [33]**); and consequently, there is no sign of the QMOs. According to a recent study **[30]**, when one of QMOs (of E2u symmetry) is half-filled, the corresponding instability may induce the Jahn-Teller distortions (JTDs) that in turn lead to the dimerization. In less distorted single-crystal Li_2RuO_3, no sign of the JTDs is seen since the formation of the zigzag chains effectively removes the orbital degeneracy or JTDs. Therefore the zigzag chains constitute an alternative state to the dimerization when the JTDs are absent. However, both the zigzag chains and dimerized lattice cost certain elastic energy that tends to stabilize uniform structure, and the prevailing state sensitively depends on details of the band structure and bulk modulus of the system (see **SM [33]** for details).

Indeed, all relevant energies vigorously compete and critically bias their mutual competition to stabilize ground states. This explains that there exist nearly degenerate states in these materials, and the prevailing ground state critically depends on details of the structure, as illustrated in **Fig. 4**. The magnetic ordering systematically decreases with increasing $(L_l-L_s)/L_s$ and eventually vanishes at a critical value where the dimerization emerges, leading to the singlet ground state observed in polycrystalline Li_2RuO_3. All results strongly indicate a direct correlation between the ground state and basal-plan distortions. The newly found Na_2RuO_3 provides a reference for almost perfect honeycomb symmetry.

The absence of the dimerization in single-crystal Li_2RuO_3 cannot be due to either impurity or quality of the single crystals. In fact, the singlet ground state is unusually

resilient to heavy impurity doping and is even enhanced by 5% Na doping (**see Fig. 3 in SM [33]**) and survives up to 50% Ir substitution for Ru in the polycrystalline samples **[31].** It is likely that the difference between the two forms of Li_2RuO_3 arises from different synthesis conditions, as discussed above, which might cause different degrees of site-disorder in the honeycomb network due to the similar ionic radius of Li and Ru, and/or slightly different stoichiometry (e.g. oxygen content) (see **SM [33]**). Hence, this work does not rule out the possibility that single-crystal Li_2RuO_3 having the same structural distortions and singlet ground state as polycrystalline Li_2RuO_3 may eventually form under certain synthesis conditions.

The work also offers the following general observations. Both Li_2RuO_3 and Li_2IrO_3 are more structurally distorted and behave with more complexities than their Na counterparts. SOC is expected to impose a J=0 state for $Ru^{4+}(4d^4)$ ions (and a $J_{eff}=1/2$ state for $Ir^{4+}(5d^5)$ ions) but the observed magnetic states in the honeycomb ruthenates as in many other ruthenates **[25]** indicate that SOC is not sufficient to induce a J=0 state. It is intriguing that all honeycomb ruthenates and iridates magnetically order in a similar temperature range (see **SM-Fig. 4 [33]**) despite the different role of SOC in them.

*Corresponding author; cao@uky.edu

References

1. G. Jackeli and G. Khaliullin, Phys. Rev. Lett. 102, 017205 (2009)

2. Y. Singh and P. Gegenwart, Phys. Rev. B 82, 064412 (2010)

3. Y. Singh, S. Manni, J. Reuther, T. Berlijn, R. Thomale, W. Ku, S. Trebst, and P. Gegenwart, Phys. Rev. Lett. 108, 127203 (2012)

4. J. Chaloupka, G. Jackeli, and G. Khaliullin, Phys. Rev. Lett. 105, 027204 (2010)

5. S. K. Choi, R. Coldea, A. N. Kolmogorov, T. Lancaster, I. I. Mazin, S. J. Blundell, P. G. Radaelli, Y. Singh, P. Gegenwart, K. R. Choi et al., Phys. Rev. Lett. 108, 127204 (2012)

6. I. Kimchi and Y.-Z. You, Phys. Rev. B 84, 180407 (2011)

7. Y.-Z. You, I Kimchi and A. Vishwanath, Phys. Rev. B 86 085145 (2012)

8. T. Hyart, A. R. Wright, G. Khaliullin, and B. Rosenow, Phys. Rev. B 85, 140510 (2012)

9. C. C. Price and N. B. Perkins, Phys. Rev. Lett. 109, 187201 (2012)

10. J. Chaloupka, G. Jackeli, and G. Khaliullin, Phys. Rev. Lett. 110, 097204 (2013)

11. H.-S. Kim, C. H. Kim, H. Jeong, H. Jin, and J. Yu, Phys. Rev. B 87, 165117 (2013)

12. S. Bhattacharjee, S.-S. Lee, and Y. B. Kim, New J. Phys. 14, 073015 (2012)

13. I. I. Mazin, H. O. Jeschke, K. Foyevtsova, R. Valenti, and D. I. Khomskii, Phys. Rev. Lett. 109, 197201 (2012)

14. X. Liu, T. Berlijn, W.-G. Yin, W. Ku, A. Tsvelik, Y.-J. Kim, H. Gretarsson, Y. Singh, P. Gegenwart, and J. P. Hill, Phys. Rev. B 83, 220403 (2011)

15. F. Ye, S. Chi, H. Cao, B. C. Chakoumakos, J. A. Fernandez-Baca, R. Custelcean, T. F. Qi, O. B. Korneta, and G. Cao, Phys. Rev. B 85, 180403 (2012)

16. H. Gretarsson, J. P. Clancy, X. Liu, J. P. Hill, E. Bozin, Y. Singh, S. Manni, P. Gegenwart, J. Kim, A. H. Said et al., Phys. Rev. Lett. 110, 076402 (2013)

17. G. Cao, T. F. Qi, L. Li, J. Terzic, V. S. Cao, S. J. Yuan, M. Tovar, G. Murthy, and R. K. Kaul, *Phys. Rev B* **88** *220414(R)* (2013)

18. I. Felner and I. Bradaric, Physica B 311, 195 (2002)

19. Yuriy Sizyuk, Craig Price, Peter Wolfle, and Natalia B. Perkins, arXiv1408.3647 (2014)

20. A. Kitaev, Ann. Phys. 321, 2 (2006)

21. Our recent neutron study found no sign of a zigzag magnetic structure in $(Na_{0.1}Li_{0.9})_2IrO_3$ by Feng Ye and G. Cao, 2014.

22. Radu Coldea, private communications (2013)

23. Johannes Reuther, Ronny Thomale and Stephan Rachel, Phys. Rev. B **90** 100405(R) (2014)

24. Gang Cao and Lance E DeLong, *"Frontiers of 4d- and 5d- Transition Metal Oxides"*, Singapore, *World Scientific* ISBN: 978-981-4374-859, June 2013

25. Giniyat Khaliullin, Phys. Rev. Lett. 111, 197201 (2013)

26. G. Chen, L. Balents, and A. P. Schnyder, Phys. Rev. Lett. 102 096406 (2009)

27. O. Nganba Meetei, William S. Cole, Mohit Randeria, Nandini Trivedi, http://arxiv.org/abs/1311.2823 (2013)

28. G. Cao, T. F. Qi, L. Li, J. Terzic, S. J. Yuan, L. E. DeLong, G. Murthy and R. K. Kaul, in *Phys. Rev. Lett*. **112**, 056402 (2014)

29. Y. Miura, Y. Yasui, M. Sato, N. Igawa, and K. Kakurai, J Phys Soc Jpn **76** 033705 (2007)

30. G. Jackeli and D. I. Khomskii, Phys. Rev. Lett. 100, 147203 (2008)

31. Simon A. J. Kimber, I. I. Mazin, Juan Shen, Harald O. Jeschke, Sergey V. Streltsov, Dimitri N. Argyriou, Roser Valenti and Daniel I. Khomskii, Phys. Rev. B **89**, 081408(R) (2014)

32. Hechang Lei, Wei-Guo Yin, Zhicheng Zhong and Hideo Hosono, Phys. Rev. B **89**, 020409(R) (2014)

33. Supplemental Material

34. Crag Price and Natalia B. Perkins, Phys. Rev. B 88, 024410 (2013)

35. O. K. Andersen and O. Jepsen, Phys. Rev. Lett. 53, 2571 (1984)

36. S.V. Streltsov, A.S. Mylnikova, A.O. Shorikov, Z.V. Pchelkina, D.I. Khomskii, and V.I. Anisimov, Phys. Rev. B 71, 245114 (2005)

37. G. Kresse and J. Furthmüller, Phys. Rev. B 54, 11169 (1996)

Captions

Fig. 1. Diffraction images in the *(h0l)* plane of the single crystal Li_2RuO_3 with space group **(a)** $P2_1/m$ and **(b)** C2/m. **Insets**: The corresponding honeycomb lattice and Ru-Ru bond distances. The temperature dependence of **(c)** the *a*-axis and **(d)** the ratio *b/a* from our single crystal $P2_1/m$ phase (blue), C2/m phase (purple), powder samples (red star), and powder data from Ref. 28 (black circles). Note that the sharp diffraction pattern clearly indicates the high quality of the single-crystal Li_2RuO_3.

Fig. 2. *Single-crystal Na_2RuO_3*: **(a)** The temperature dependence of the magnetic susceptibility for the basal plane χ (T) and out-of-plane $\chi_\perp$(T) for single-crystal Na_2RuO_3; Right scale: $1/\Delta\chi$ where $\Delta\chi = \chi - \chi$ and χ is the temperature-independent contribution to χ. **(b)** The temperature dependence of the specific heat C(T) and $\chi_\perp$(T) (right scale) for.

Fig. 3. *Single-crystal Li_2RuO_3 (C)*: The temperature dependence of **(a)** the magnetic susceptibility χ (T) and $\chi_\perp$(T) and $1/\Delta\chi_\perp$ (right scale) for $1.7 < T < 850$ K and **(b)** the specific heat C(T) and $\chi_|$ (T) and $\chi_\perp$(T) (right scale) at low T. *Single-crystal Li_2RuO_3 (P)*: The temperature dependence of **(c)** χ (T) and $\chi_\perp$(T) and $1/\Delta\chi_\perp$ (Inset) and **(d)** $\chi_|$ (T) and $\chi_\perp$(T) and $d\chi_\perp/dT$ (right scale) at low T.

Fig. 4. The Neèl temperature T_N as a function of the bond distance ratio $(L_l - L_s)/L_s$ for
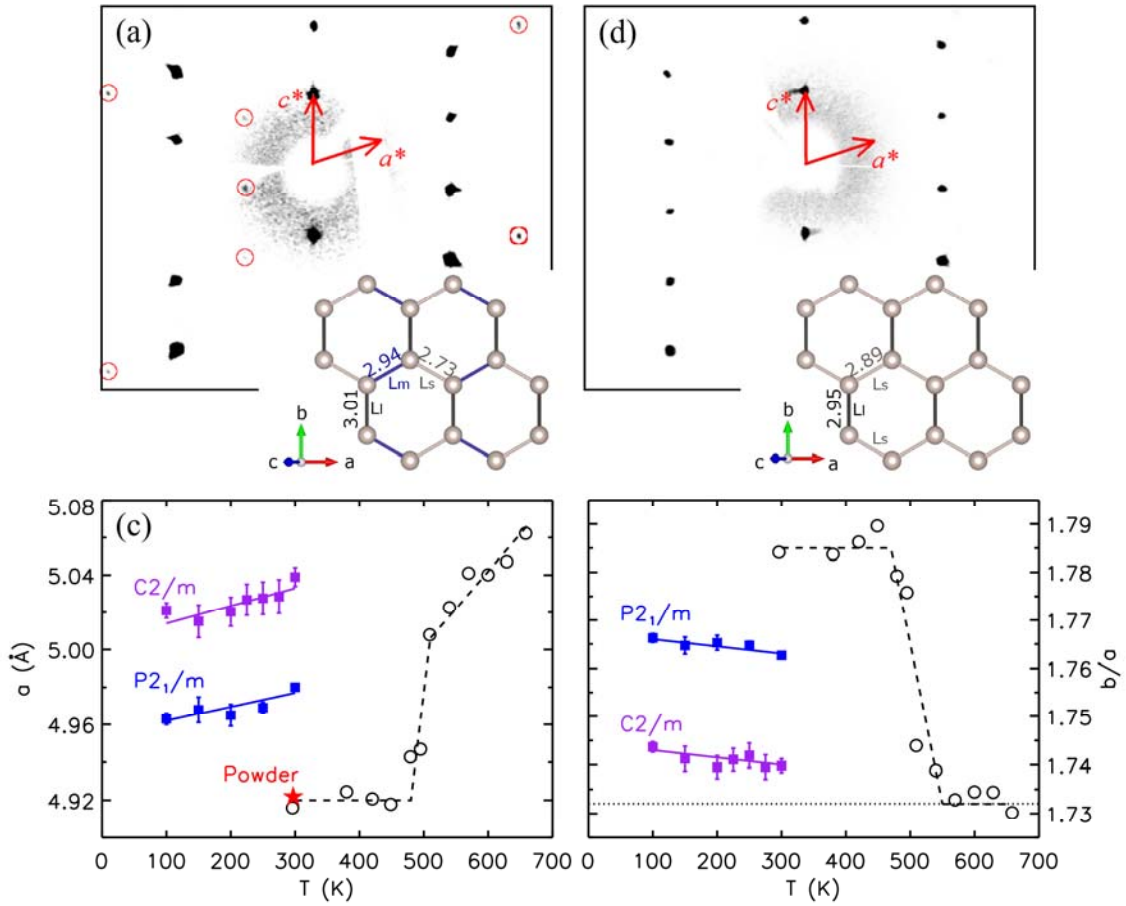
all honeycomb ruthenates. Inset: a schematic of the honeycomb lattice featuring L_l and L_s.
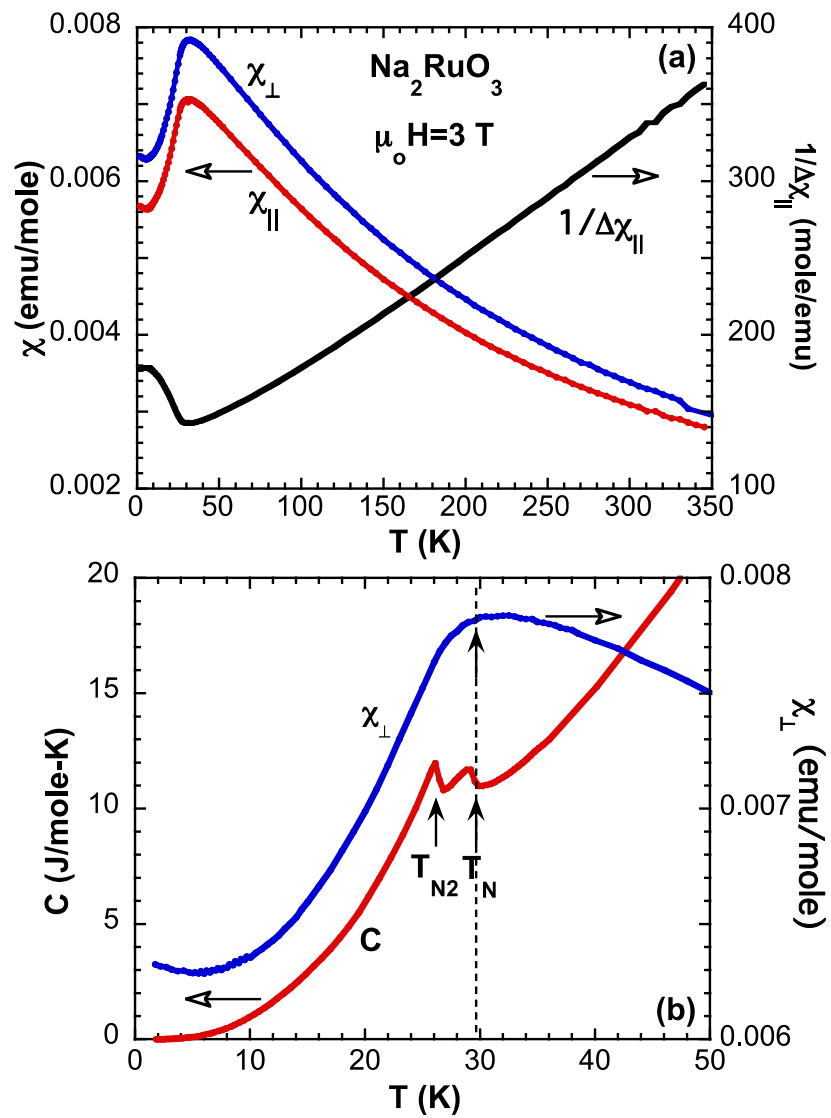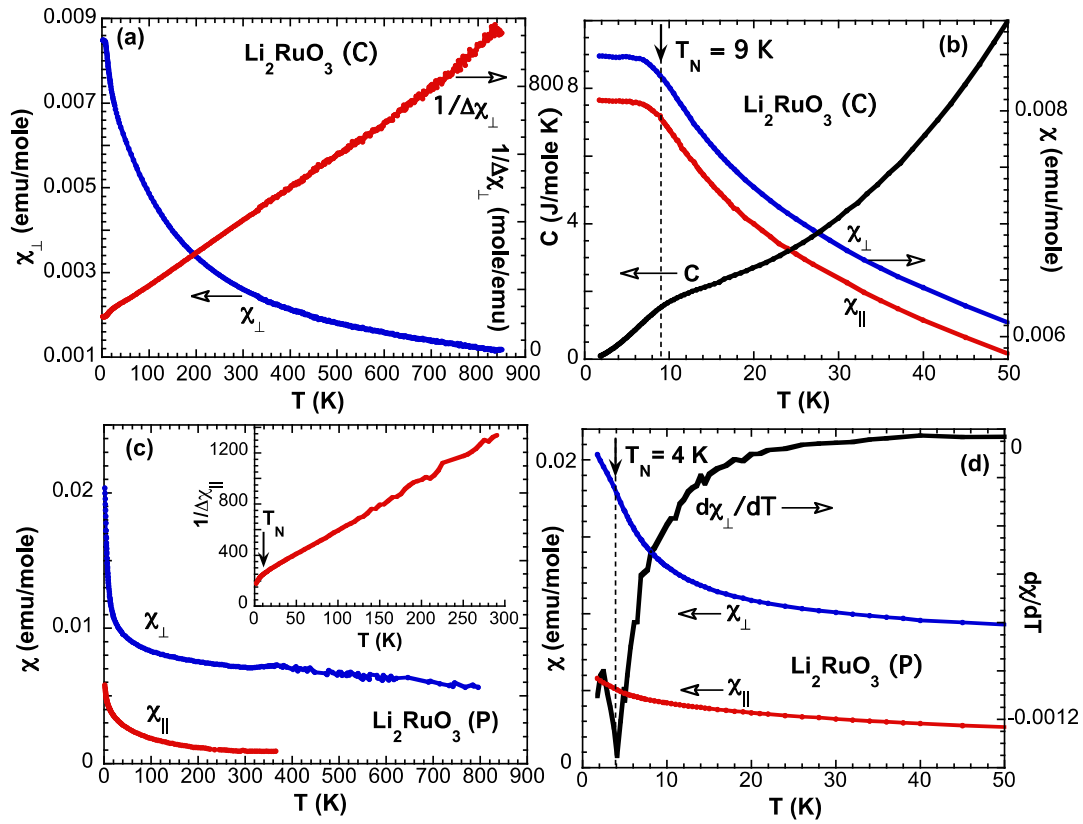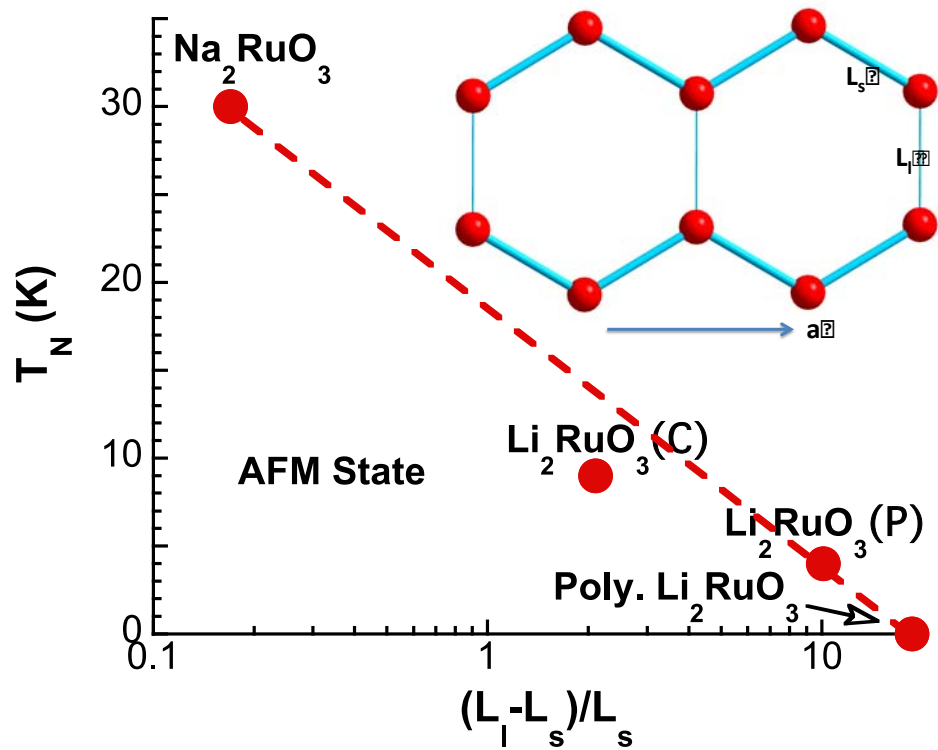

Fig. 1

Fig. 2

Fig. 3

Fig. 4